Talin and Vinculin Play Distinct Roles in Filopodial Motility in the Neuronal Growth Cone

Anne M. Sydor, Anne L. Su, Feng-Song Wang, Alian Xu, and Daniel G. Jay

Department of Molecular and Cellular Biology, and the Neuroscience Program, Harvard University, Cambridge, Massachusetts 02138

Abstract. Filopodial motility is critical for many biological processes, particularly for axon guidance. This motility is based on altering the F-actin–based cytoskeleton, but the mechanisms of how this occurs and the actin-associated proteins that function in this process remain unclear. We investigated two of these proteins found in filopodia, talin and vinculin, by inactivating them in subregions of chick dorsal root ganglia neuronal growth cones and by observing subsequent behavior by video-enhanced microscopy and quantitative morphometry. Microscale chromophore-assisted laser inactivation of talin resulted in the temporary cessation of filopodial extension and retraction. Inactivation of vinculin caused an increased incidence of filopodial bending and buckling within the laser spot but had no effect on extension or retraction. These findings show that talin acts in filopodial motility and may couple both extension and retraction to actin dynamics. They also suggest that vinculin is not required for filopodial extension and retraction but plays a role in the structural integrity of filopodia.

A major challenge in cell biology is understanding the molecular mechanisms of cell motility. This is particularly true for understanding the formation of the nervous system as the neuronal growth cone responds to signals in its environment by directed filopodial motility. The direction of growth cone motility can be altered by a single filopodial contact (O'Connor et al., 1990). Moreover, filopodial elimination by cytochalasin disorients growth cone pathfinding in vitro (Marsh and Letourneau, 1984; Zheng et al., 1996) and in vivo (Bentley and Toroian-Raymond, 1986; Chien et al., 1993).

Filopodia are densely filled with bundled F-actin (Yamada et al., 1970), and it is thought that the interaction of actin-associated proteins is required for their motility. Some of these proteins can bundle F-actin, as required for the parallel actin filaments found in filopodia (Stossel, 1993). Others may function to attach F-actin to macromolecular complexes such as focal contacts during motility (Burridge et al., 1988). Many actin-associated proteins have been identified in the growth cone, but it has thus far been difficult to demonstrate a functional role for any of these proteins inside neuronal growth cones (Letourneau, 1992). We are particularly interested in finding proteins that might serve to connect F-actin to the membrane and ultimately to the external environment. Talin and vinculin are good candidates to play such a role.

Talin is a 270-kD protein that binds to F-actin, the β_1 subunit of the integrin receptor (Horwitz et al., 1986), α-actinin, and vinculin in vitro (Burridge and Mangeat, 1984; Gilmore et al., 1993). It colocalizes with these proteins in fibroblast focal adhesion plaques (Samuelsson et al., 1993), and microinjection of polyclonal antibodies to talin decreases fibroblast motility (Nuckolls et al., 1992). It is found in chick dorsal root ganglia (DRG)[1] neuronal growth cones (Letourneau and Shattuck, 1989) where it localizes to focal contacts (Letourneau and Gomez, 1996).

Vinculin, a 117-kD protein, is also a major component of focal contacts (Burridge et al., 1988) and is found in neuronal growth cones (Letourneau and Shattuck, 1989). Vinculin binds to talin (Burridge and Mangeat, 1984), F-actin (Johnson and Craig, 1995), and α-actinin (Wachsstock et al., 1987) in vitro. It colocalizes with these proteins and the β_1 subunit of the integrin receptor in fibroblasts (Samuelsson et al., 1993). Studies have implicated a role for vinculin in adhesion or motility in fibroblasts (Westmeyer et al., 1991; Rodriguez-Fernandez et al., 1992, 1993) and PC12 cells (Varnum-Finney and Reichardt, 1994).

While much is known about the in vitro properties of talin and vinculin, what they do in cells remains unclear. This is particularly true for neurons for which functional perturbation studies have been difficult. Although previous investigations have generated chronic functional perturbations of these proteins in other cell types (Nuckolls et al., 1992; Varnum-Finney and Reichardt, 1994), these

---

1. *Abbreviations used in this paper:* DRG, dorsal root ganglia, HBBS, Hanks' balanced buffered saline; MG, malachite green; micro-CALI, microscale chromophore-assisted laser inactivation.

studies could not directly address the dynamic function of talin and vinculin during motility.

We have addressed the role of talin and vinculin in filopodia by generating the acute and localized loss of these proteins using microscale chromophore-assisted laser inactivation of protein function (micro-CALI) (Diamond et al., 1993). Micro-CALI functionally inactivates proteins of interest within a 10-μm spot by targeting a laser microbeam of a wavelength not absorbed by most cellular components (620 nm) to the protein of interest via a nonblocking antibody labeled with the chromophore malachite green (MG) (Jay, 1988). Laser excitation of the chromophore generates short-lived free radicals that damage proteins within 15 Å of the dye molecules (Liao et al., 1994). CALI is selective for the bound protein even in multiprotein complexes (Linden et al., 1992; Liao et al., 1995) and has precisely phenocopied genetic loss of function mutations in all cases tested (Beermann and Jay, 1994). Micro-CALI was recently applied to focally inactivate calcineurin in DRG growth cones, resulting in a local retraction of filopodia (Chang et al., 1995). Here we report our experiments that address the molecular mechanisms of filopodial motility, by focally inactivating talin and vinculin using micro-CALI.

Materials and Methods

Antibodies

mAb 8d4, which recognizes talin (Otey et al., 1990), mAb VIN 11.5, which recognizes vinculin (Westmeyer et al., 1990), and purified mouse IgG (nonimmune) were purchased from Sigma Chemical Co. (St. Louis, MO). VIN 11.5 was further purified by protein A chromatography. Antibodies were labeled with malachite green isothiocyanate (Molecular Probes, Inc., Eugene, OR) to a ratio of six to eight dye moieties per protein molecule by the method of Jay (1988). Fluorescent secondary antibodies were purchased from Cappel Laboratories (Malvern, PA).

Neuronal Culture

DRG neurons from E9–12 chick embryos (Spafas, Inc., Norwich, CT) were dissociated and cultured as modified from Bray (1991). DRGs were placed in 0.25% trypsin (in Hanks' balanced buffered saline [HBBS] without Ca²⁺ and Mg²⁺; GIBCO BRL, Gaithersburg, MD) at 37°C for 15 min and dissociated using a p200 Pipetteman (Rainin Instrument Co., Inc., Woburn, MA). Cells were washed in supplemented L15 media (standard DRG neuronal media with 25 ng/ml NGF [7S; Boehringer Mannheim Biochemicals, Indianapolis, IN] and 10% FBS [Sigma Chemical Co.]), plated onto poly-L-lysine– (1 mg/ml) and laminin– (0.1 mg/ml) coated coverslips, and incubated at 37°C in supplemented L15 media.

Immunoblotting

Immunoblot analyses were performed according to Dubreuil et al. (1987). In brief, E11 chick DRGs were lysed in 50 μl of a buffer containing 0.5% Triton X-100 and a protease inhibitor cocktail (Boehringer Mannheim Biochemicals) and vortexed, and 2× gel sample buffer was added. Samples of DRGs (2.5 DRGs per lane) were then electrophoresed on 7% SDS-PAGE minigels and electrophoretically transferred to nitrocellulose. The nitrocellulose blots were blocked with 10% nonfat dry milk, incubated for 3 h at room temperature with 1 μg/ml VIN.11 anti-vinculin or 8d4 anti-talin mAbs, and probed with alkaline phosphatase-labeled goat anti–mouse IgG antibodies (1:500) for 1 h at room temperature. Blots were then developed in alkaline phosphatase substrate (Sigma Chemical Co.).

Immunocytochemistry

Cultured E12 chick DRG neurons on glass coverslips were fixed for 10 min with 4% formaldehyde (freshly made from paraformaldehyde) and 400 mM sucrose in PBS as modified from Letourneau and Shattuck (1989). After fixation, cells were permeabilized for 5 min with 0.5% Triton X-100 in PBS. After three gentle washes in PBS, cells were incubated for 30 min in blocking buffer (PBS with 10% goat serum), followed by primary antibody diluted in blocking buffer at 4°C overnight. After three rinses in PBS, cells were probed with FITC-conjugated secondary antibodies (1:50) and rhodamine-phalloidin (0.66 μM final; Molecular Probes, Inc.) diluted in blocking buffer for 1 h at room temperature. After three rinses in PBS, cells were mounted in Fluoromount-G (Southern Biotechnology Associates, Inc., Birmingham, AL) and viewed using a confocal microscope (LSM 410; Carl Zeiss, Inc., Thornwood, NY).

Antibody Loading by Trituration

Malachite green–labeled antibodies were loaded into DRG neurons by a modified trituration method (Borasio et al., 1989; Clarke and McNeil, 1992). After incubation in 0.25% trypsin (in HBBS without Ca²⁺ and Mg²⁺) at 37°C for 15 min, as described above, DRGs were placed in 50 μl of the desired antibody solution at concentrations between 1 and 1.8 mg/ml in HBBS. DRGs were drawn up and down in yellow Pipetteman tips using a p200 micropipetteman until there was a uniform suspension of single cells (~100 strokes). This is thought to create temporary holes in the cell membranes (Clarke and McNeil, 1992), enabling antibodies to enter the cells. To visualize loading, FITC-conjugated rabbit IgG (1 mg/ml) was included in the antibody solution during trituration. After trituration, cells were centrifuged twice for 10 s at 2,000 rpm (IEC clinical centrifuge; International Equipment Co., Needham Heights, MA) to remove the antibody solution, gently suspended in supplemented L15 media, and plated, as described previously. These loaded DRG neurons were then used for micro-CALI.

To compare loading and cytoskeletal retention, loaded neurons were either fixed and extracted as decribed above or they were extracted for 3 min with 0.05% Triton X-100, 60 mM Pipes, 25 mM Hepes, 10 mM EGTA, and 2 mM MgCl₂ at 37°C (Letourneau, 1983) before fixation. Cells were then probed with 1:50 FITC-conjugated goat anti–mouse IgG (H + L) and 0.66 μM rhodamine-phalloidin at room temperature for 2 h, rinsed, mounted, and viewed as described above.

Micro-CALI of Proteins in Growth Cones

Micro-CALI was performed as described previously (Diamond et al., 1993; Chang et al., 1995). DRG neuronal cultures were kept at 37°C with a stage incubator (Opti-Quip Inc., Highland Mills, NY) throughout the experiment. Micro-CALI was performed from 1 to 6 h after plating to ensure that the neurons were still loaded with antibodies. In a typical micro-CALI experiment, neurons were briefly observed by epifluorescence to verify antibody loading. A chosen growth cone was first observed using phase-contrast optics for 5 min, and then a region of the growth cone was laser irradiated for 5 min (λ = 620 nm, τ = 3.5 ns, 30 μJ per pulse at 20 Hz) using a nitrogen-driven dye laser (model VSL-337; Laser Science Inc., Newton, MA). Growth cones were observed during irradiation, and for an additional 5 min, by time-lapse video microscopy (every 15 s) using custom-written software (Jay and Keshishian, 1990) and an optical memory disc recorder (Panasonic, Secaucus, NJ).

Methods of Quantitation

Growth cone parameters measured were bending/buckling of filopodia, filopodial number, and the rates of filopodial motility and neurite outgrowth. Quantitation was done using NIH Scion Imaging System software (Scion Co., Frederick, MD) and analyzed using Cricket Graph software (Malvern, PA) and Minitab Statistics software (Pennsylvania State University) (significance level of $P < 0.05$). Filopodial length was measured in every frame of the time-lapse period. The rates of extension and retraction were obtained by taking the first derivatives of these plots. A growth cone was scored as having a cessation in motility only if the rates of irradiated filopodia for that growth cone dropped to 0.0 ± 0.2 μm/min for >1 min in the irradiated area. No bias in selecting filopodia for irradiation occurred; the rates of the filopodial motility inside and outside the laser spot were compared before irradiation to ensure that they were statistically indistinguishable. Filopodial bending was defined as a single angular event (>15°), and buckling was defined as two or more angular events in a filopodium often accompanied by loss of attachment to the substratum. Most of the data were analyzed double blind to ensure objective scoring of parameters; data sets done without double-blind analysis showed similar results.

Results

Talin and Vinculin Antibodies Are Loaded into Chick DRG Neuronal Growth Cones

We confirmed that our antibodies recognized talin and vinculin by immunoblotting (Fig. 1) and by indirect immunocytochemistry (Figs. 2 and 3). Immunoblotting with VIN.11 of DRG cell lysates showed a predominant band with an apparent molecular mass of 117 kD, which corresponds to the molecular mass of vinculin (Fig. 1, lane *a*). Immunoblotting with 8d4 recognized a 230-kD species that corresponds to the molecular mass of talin, but several other bands were detected including a major 80-kD band (Fig. 1, lane *b*). These other bands are very likely to be proteolytic fragments of talin. Immunoblotting using a different anti-talin antibody recognizes the same bands (data not shown). Furthermore, talin is very susceptible to proteolysis (Molony et al., 1987), and immunoblotting of a preparation of purified talin that had been stored at 4°C showed bands of similar size.

Immunocytochemistry using 8d4 and VIN.11 showed patterns of talin and vinculin expression within DRG growth cones after extraction similar to those seen by Letourneau and Shattuck (1989). Double labeling with rhodamine-phalloidin to reveal microfilaments shows significant colocalization with 8d4 anti-talin (Fig. 2, *a–d*) and, to a lesser extent, with anti-vinculin (Fig. 2, *e–h*). The pattern of talin localization is punctate, suggesting that talin resides in focal contacts and clearly extends to filopodia. Vinculin expression was concentrated in the main body of the growth cone but also extended into the filopodia.

To inactivate these proteins using CALI, it was necessary to load dye-labeled antibodies into the neuronal growth cones. Chick DRG neurons were loaded with antibodies by trituration. Typically, 50% of the neurons survive, and of these, >80% had antibodies that were retained with a half-life of 12 h (Sydor, A.M., unpublished results).
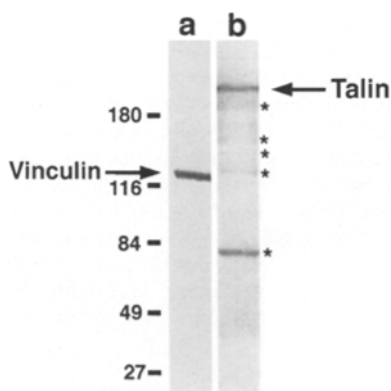

Figure 1. Specificity of antibodies by immunoblotting. Immunoblot analysis confirms that VIN.11 recognizes a single predominant species in DRG neuronal lysates with the apparent molecular mass of vinculin (*arrow*, lane *a*). 8d4 recognizes a band at 230 kD corresponding to the molecular mass of talin (*arrow*, lane *b*) but also recognizes several other bands (*) that are likely to be proteolytic fragments, as talin is very susceptible to cleavage in cell lysates.

We verified that the antibodies were loaded and retained in growth cones by immunocytochemistry of fixed and detergent-extracted neurons using secondary antibody alone (Fig. 3). Anti-talin, anti-vinculin, and nonimmune mouse IgG immunoreactivity were detected in the growth cone of trituration-loaded DRG neurons. All three antibodies were found in the growth cone of neurons that were fixed and then extracted, and the staining extended out to the filopodia. Both talin and vinculin staining were retained in neurons that had been extracted before fixation and had significant overlap with rhodamine-phalloidin staining, showing an association of anti-talin and anti-vinculin antibodies with the F-actin cytoskeleton. These patterns were similar to those observed by indirect immunocytochemistry (Fig. 2; Letourneau and Shattuck, 1989). In contrast, neurons loaded with nonimmune IgG showed uniform staining, showing that IgG was present in the growth cone and filopodia, but upon extraction, this staining was lost, showing that this nonspecific antibody did not associate with the cytoskeleton. Control cells stained with secondary antibody alone did not display detectable staining (data not shown). Together, these findings show that trituration introduces these antibodies into DRG neuronal growth cones, and the antibodies specifically recognize their respective antigens.

Antibody Loading Has No Effect on Growth Cone Motility

Loading of MG-8d4, MG-VIN11.5, or MG-nonimmune IgG into DRG neurons did not affect the rate of neurite outgrowth (Fig. 4 *a*), filopodial number (Fig. 4 *b*), or filopodial motility (Table I). Growth cone morphology was not affected by trituration loading of these antibodies. Neurons extended long, healthy neurites, and neurite number and length were similar for all conditions observed for up to 2 d (data not shown). We also loaded MG-BSA into DRG neurons or carried out trituration without added protein (mock loaded), and no significant effect was observed for the measured parameters (Fig. 4).

Micro-CALI of Talin But Not Vinculin Stalls Filopodial Motility

We locally inactivated talin by laser irradiating regions of growth cones (Fig. 5 *a*, *circle*; t = 0:00) loaded with malachite green–labeled antibodies to talin (MG–anti-talin). This caused filopodia in the irradiated region to stall, ceasing extension, retraction, and lateral movement for 2–5 min (Fig. 5 *a*; compare *arrow* in t = 2:00 with t = 7:15). After that time, motility was recovered (t = 7:45). Filopodia outside the area of irradiation showed no change in motility. The cessation of filopodial motility occurred in 80% (*n* = 31) of neurons treated with micro-CALI of talin, and this behavior was rarely seen with neurons grown on uniform permissive substrates. Lamellipodia within the laser spot occasionally showed a slight retraction when laser light was initiated, but recovered within a few seconds and showed normal dynamic motility thereafter.

The loss of filopodial dynamics is clearly illustrated by plotting the rates of change in filopodial length vs time (Fig. 6, *a* and *b*; *graphs*). Before laser irradiation, these rates varied substantially for all filopodia. 2 min after laser
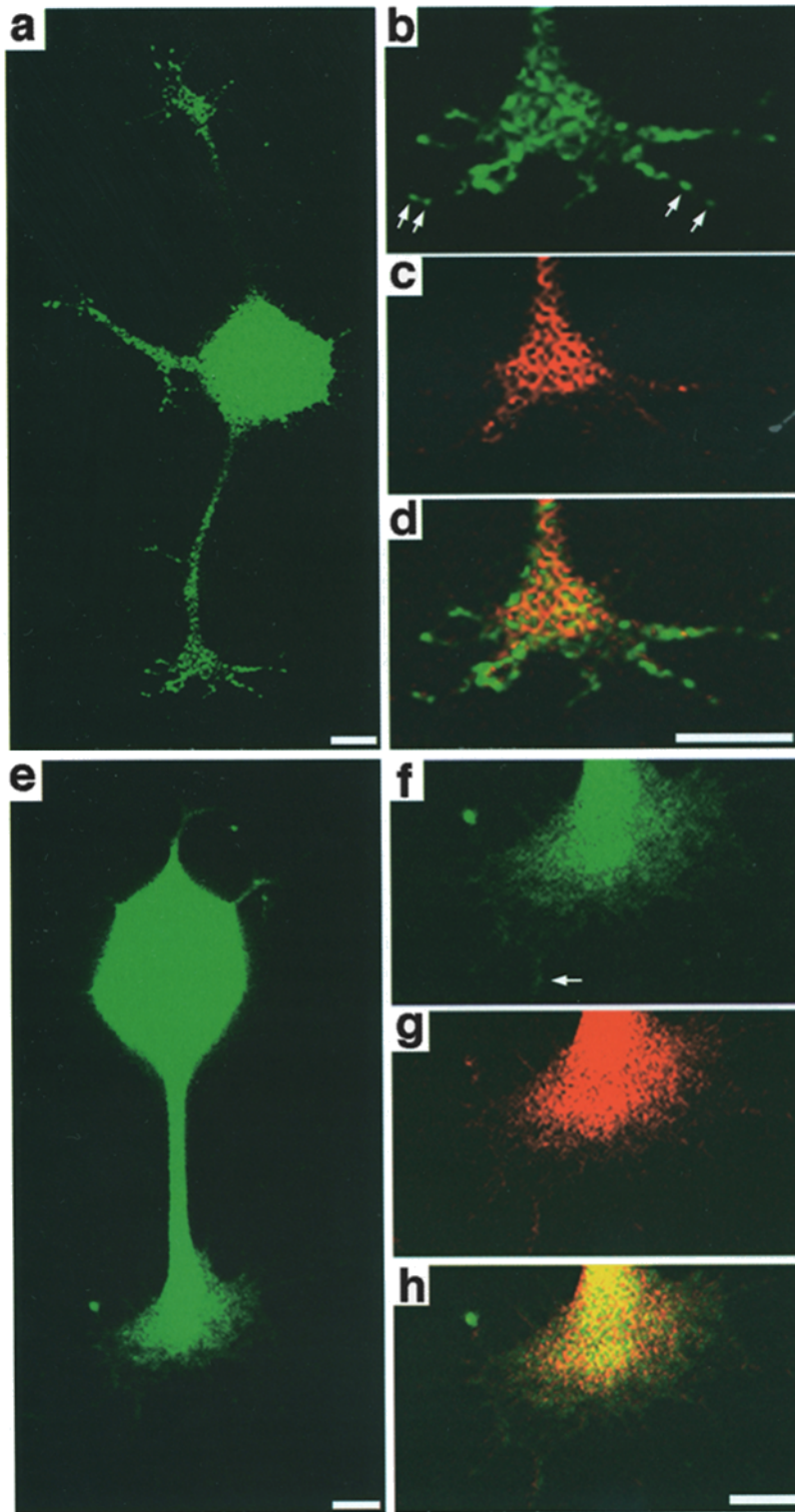
Figure 2. Anti-talin and anti-vinculin recognize cytoskeletally associated antigens. Indirect immunocytochemistry confirms that 8d4, an anti-talin mAb, stains chick DRG neuronal growth cones (*green* in *a, b,* and *d*). Note that talin staining shows a punctate pattern that extends into filopodia (*double arrows*). Talin colocalizes with F-actin as shown in *d* (*yellow*) by superimposing the images presented in *b* with the rhodamine-phalloidin fluorescence shown in *c* (*red*). (*b–d*) Close-ups of the lower growth cone in *a.* (*e–h*) Immunolocalization of vinculin using VIN.11, an anti-vinculin mAb, showing that vinculin is primarily localized in the growth cone body (*green* in *e* and *f*) but also extends to the filopodia (*f, arrow*). (*f–h*) Close-up of the growth cone in *e.* Vinculin was also shown to colocalize with F-actin (*yellow* in *h*) by superimposing the image in *f* with the rhodamine-phalloidin fluorescence image (*red* in *g*). Bar, 10 μm.

irradiation had begun, the rates of change in filopodial length for irradiated filopodia dropped to 0.0 ± 0.2 μm/min and recovered after 2–5 min (Fig. 6 *a*). Filopodia that were not laser irradiated showed no apparent change in the rates of extension and retraction throughout the time-lapse period (Fig. 6 *b*).

In contrast, micro-CALI of vinculin had no effect on filopodial extension and retraction within the laser spot (Fig. 5 *b*, *circle*; t = 0:00) or outside the spot (Figs. 5 *b* and 6, *c* and *d*). As vinculin binds to talin in focal contacts, these results act as a negative control, supporting the specificity of the inactivation of talin. We also tested for nonspecific effects of laser irradiation on control cells loaded with a malachite green–labeled nonimmune antibody
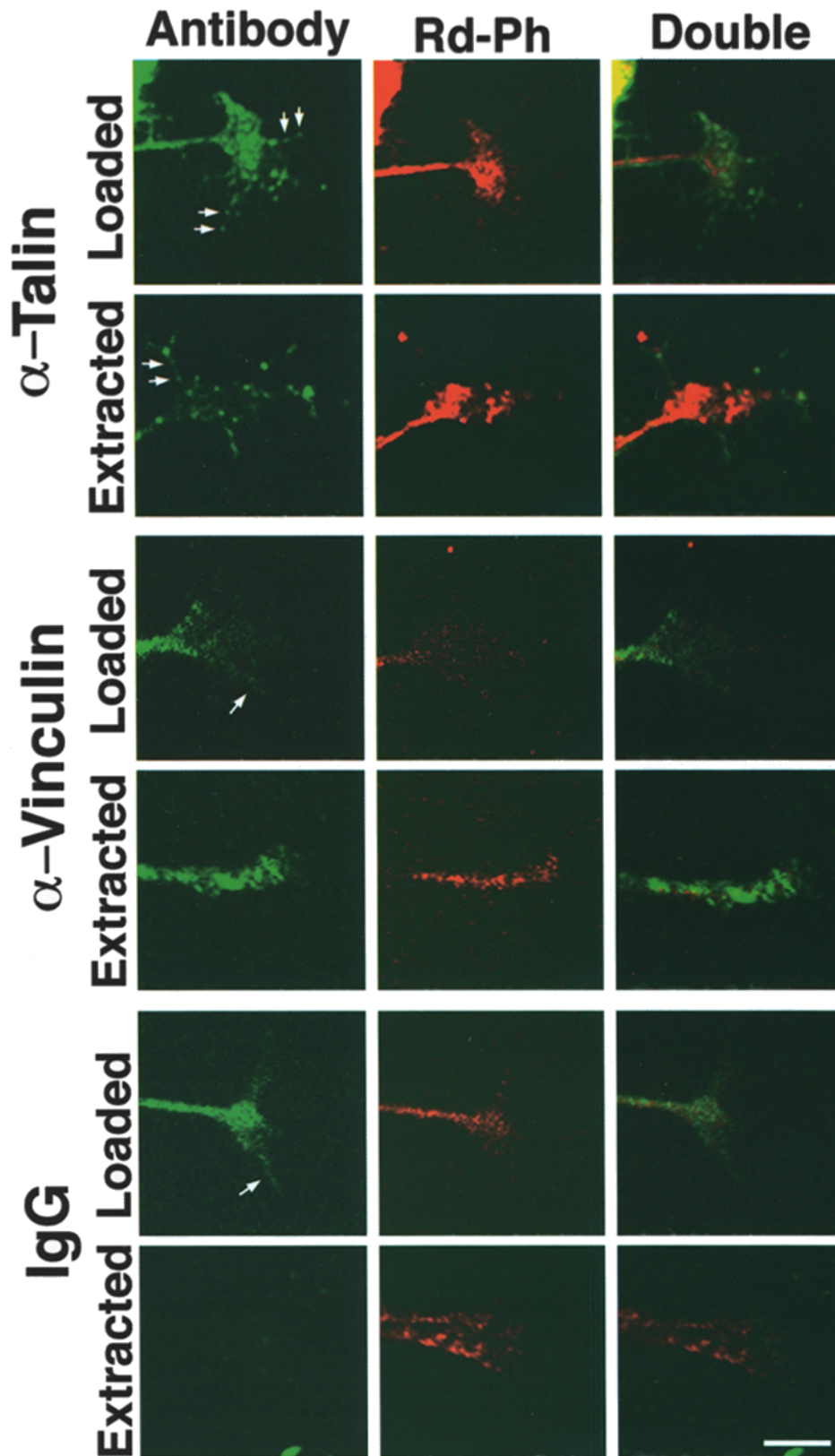
Figure 3. Trituration loading of antibodies into chick DRG neurons and their retention. Immunocytochemistry of antibody-loaded chick DRG neurons using FITC secondary antibodies confirms trituration loading of antibodies into DRG neuronal growth cones, and that these antibodies are retained by the cytoskeleton. Chick DRG neurons that were trituration loaded with 8d4 (*α-Talin*), VIN11.5 (*α-Vinculin*), or nonimmune IgG (*IgG*) were fixed before detergent extraction (*Loaded*), or detergent-extracted before fixation (*Extracted*) to show cytoskeletal retention of antibodies, and subsequently probed with FITC-labeled secondary antibodies and rhodamine-phalloidin. Note that all trituration-loaded antibodies reach growth cone filopodia, but only anti-talin and anti-vinculin antibodies are retained after extraction. Moreover, double labeling with these antibodies and rhodamine-phalloidin (*Rd-Ph*) show overlap, suggesting that these anti-talin and anti-vinculin colocalize with the cytoskeleton (*Double*). Malachite green labeling of antibodies had no effect on trituration efficiency or in antigen recognition (data not shown). (*Arrows*) Filopodia. Bar, 10 μm.

(MG-IgG). All filopodia remained dynamic throughout the 15-min time-lapse recording (Figs. 5 *c* and 6, *e* and *f*). Laser excitation of MG-IgG had no effect on filopodial movement, growth cone behavior, or neurite outgrowth.

Localized inactivation of talin caused a regional loss of filopodial extension and retraction that was significantly different ($P < 0.001$) than all other treatments (Table I). There was a significant drop in the rate of filopodial exten-
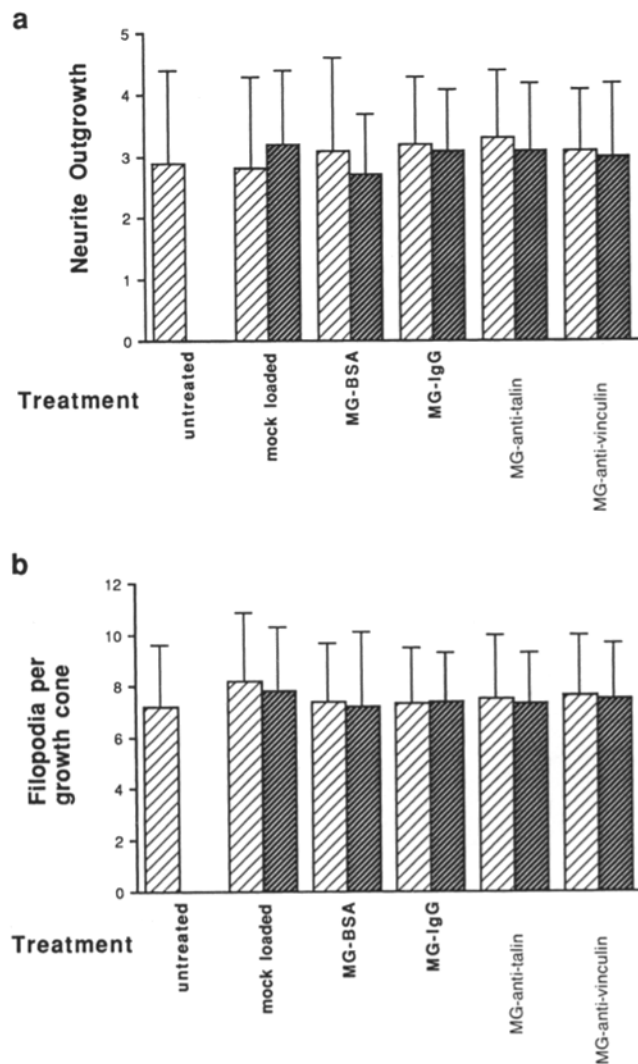
a

b

Figure 4. Antibody loading and micro-CALI of talin and vinculin does not affect neurite outgrowth or filopodial number. Neither loading of dye-labeled proteins (*MG-BSA*, n = 12; *MG-IgG*, n = 22; *MG-anti-talin*, n = 31; *MG-anti-vinculin*, n = 18) nor the harsh trituration used for loading (*mock loaded*; n = 10) caused significant differences in rate of neurite outgrowth in μm per 5 min (*a*) or number of filopodia per growth cone (*b*), compared to unloaded controls that were dissociated more gently (*untreated*; n = 12). Moreover, laser irradiation of the growth cones of these treated neurons also had no significant effect on these parameters (zM test used to measure significance). (*Light bars*) Data for neurons that were not laser irradiated; (*dark bars*) data for loaded neurons subjected to 5 min of laser irradiation using the micro-CALI apparatus.

sion and retraction only for filopodia within the laser spot during micro-CALI of talin (marked by *), and no significant effect was observed when CALI was carried out with MG–anti-vinculin or nonimmune IgG (Table I). The average filopodial motility did not drop to zero because 20% of the growth cones was not affected and also because the duration of stalling and the time of recovery of motility varied between growth cones. CALI of talin and vinculin had no significant effect on other growth cone parameters

such as neurite outgrowth or filopodial number (Fig. 4, *a* and *b*).

Micro-CALI of Vinculin Causes Filopodial Bending and Buckling

Filopodia treated with micro-CALI of vinculin had a greater tendency to bend or buckle (Fig. 5 *b*, *arrow*; t = 7:15). Summation analysis of all growth cones tested showed that micro-CALI of vinculin resulted in an increased rate of bending and buckling of filopodia (Fig. 7). The percentages of bending or buckling filopodia of growth cones, correlated with respect to the time of initiation of laser irradiation, were summed and plotted against time. Growth cones normally have a small number of bent or buckled filopodia, and the baseline percentage of bent or buckled filopodia is 10 ± 1% as observed in the graph of unirradiated filopodia (Fig. 7, *b*, *d*, and *f*).

Filopodia subjected to micro-CALI of vinculin within the laser spot showed a more than threefold increase in the percentage of bending or buckling during the lasing period (Fig. 7 *a*). The time of half-maximal response is ~2.5 min and peaks at 5 min (the end of laser irradiation). This incidence decreases after lasing and has returned almost to baseline by 10 min after laser initiation. Unirradiated filopodia were unaffected (Fig. 7 *b*), and laser irradiation of neurons loaded with MG–anti-talin or MG-IgG did not affect filopodial bending and buckling (Fig. 7, *c–f*). These data show that micro-CALI of vinculin caused increased filopodial bending and buckling, a different effect from that observed after micro-CALI of talin.

Discussion

Most of what is known about talin and vinculin has been gained from in vitro approaches (Burridge et al., 1988) or by chronic loss of function (e.g., Nuckolls et al., 1992; Varnum-Finney and Reichardt, 1995). Hypotheses regarding the dynamic roles of these proteins must be tested inside living cells. We have used micro-CALI to locally and acutely inactivate talin and vinculin to address their functions in chick DRG neuronal growth cone motility. Micro-CALI of talin caused filopodial stalling; micro-CALI of vinculin resulted in increased filopodial bending or buckling. These findings suggest that talin and not vinculin serves to connect F-actin to the membrane and ultimately to the external environment.

Nuckolls et al. (1992) showed that microinjection of polyclonal antibodies against talin into fibroblasts decreased the rate of wound healing. Our findings extend this work to implicate talin in a specific role in cell motility, namely filopodial extension and retraction. Moreover, our findings coupled with the observation that talin can simultaneously bind F-actin and β_1 subunit of integrin in vitro (Burridge and Mangeat, 1984), and the localization of talin at focal contacts in growth cone filopodia (Figs. 2 and 3; Letourneau and Gomez, 1996; Letourneau and Shattuck, 1989) suggests that talin couples F-actin to the substratum during filopodial motility. Our findings do not address the movement of unattached filopodia. The vast majority of filopodia that could be observed throughout the time course were attached to the substratum. As the

Table I. Micro-CALI of Talin Decreases the Rate of Filopodial Extension and Retraction

	Rate of filopodial extension and retraction					
	Pre-laser		During laser		Post-laser	
Treatment	Unirradiated filopodia	Irradiated filopodia	Unirradiated filopodia	Irradiated filopodia	Unirradiated filopodia	Irradiated filopodia
	μm/min					
Untreated (n = 12 cells)	10.8 ± 2.2	N/A	N/A	N/A	N/A	N/A
MG-IgG loaded (n = 22 cells)	10.8 ± 2.6	11.4 ± 2.4	10.7 ± 2.9	10.6 ± 3.0	10.2 ± 2.65	10.5 ± 2.8
MG–anti-talin loaded (n = 31 cells)	10.6 ± 2.8	10.4 ± 2.9	10.1 ± 2.1	4.3 ± 2.4*	10.4 ± 2.1	10.0 ± 2.2
MG–anti-vinculin loaded (n = 18)	10.5 ± 2.4	10.4 ± 2.8	10.6 ± 2.9	10.6 ± 2.2	10.4 ± 2.4	10.7 ± 2.6

Average filopodial motility was compared for filopodia inside and outside the laser-irradiated spot for DRG neuronal growth cones subjected to micro-CALI. Trituration loading of malachite green–labeled antibodies to talin (MG–anti-talin) or vinculin (MG–anti-vinculin) alone caused no significant change in the average rate of filopodial motility compared with nonimmune MG-IgG loaded and untreated controls (compare pre-laser values). Micro-CALI of talin but not vinculin caused a significant transient decrease in the average rate of filopodial motility only within the laser spot, as compared with all other controls (compare during laser values). Significance was measured by the zM test; *, $P < 0.001$.
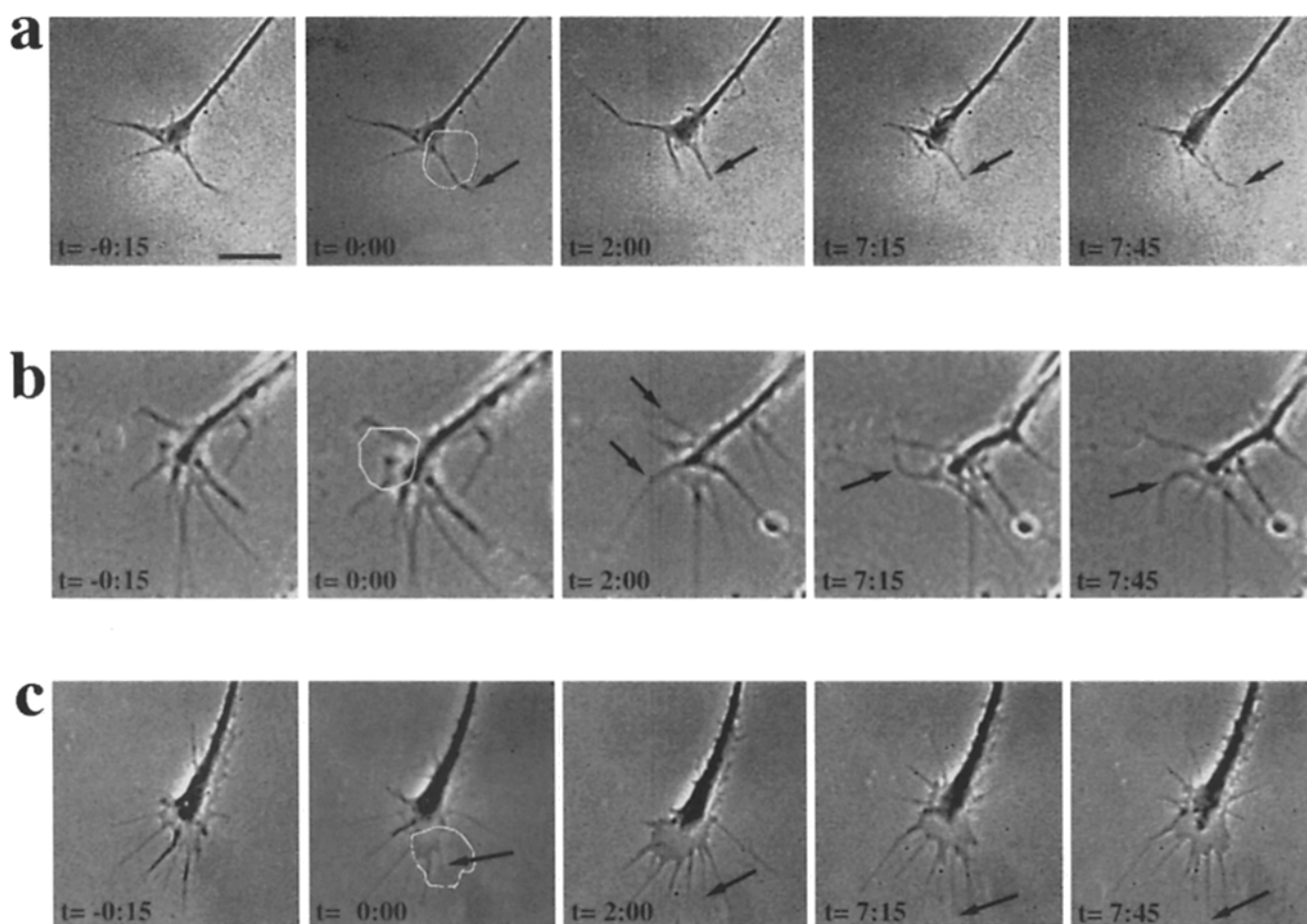

Figure 5. Micro-CALI of talin and vinculin cause distinct effects on filopodia. Time-lapse micrographs of chick DRG neurons subjected to micro-CALI of talin (a), micro-CALI of vinculin (b), and laser irradiation of a neuron loaded with MG-nonimmune IgG (c). The laser spot is shown by the white circle at time zero; all other times are relative to the onset of laser irradiation. (a) Micro-CALI of talin caused a loss of filopodial motility. 2 min after laser irradiation began, filopodia within the laser spot (arrow) stopped moving (t = 2:00). The loss of movement lasted for 5.25 min (t = 7:15), after which time, motility was recovered (t = 7:45). This loss of motility was not seen after micro-CALI of vinculin (b) or MG-IgG controls. (b) Micro-CALI of vinculin causes an increase in filopodial bending and buckling. Filopodia continued to move throughout the time-lapse sequence. However, filopodia within the laser spot bent frequently (arrows in t = 2:00, 7:15, 7:45), which was not true of micro-CALI against talin (a) or MG-IgG controls (c). These images were taken with the growth cone and neurite slightly out of focus. This was done to visualize the bent filopodia that are out of the focal plane of the rest of the neurite. (c) Micro-CALI of MG-IgG controls do not affect filopodia. Filopodia within the laser spot (arrows) continued to move throughout the time lapse and showed no increase in bending and buckling. Bar, 10 μm.
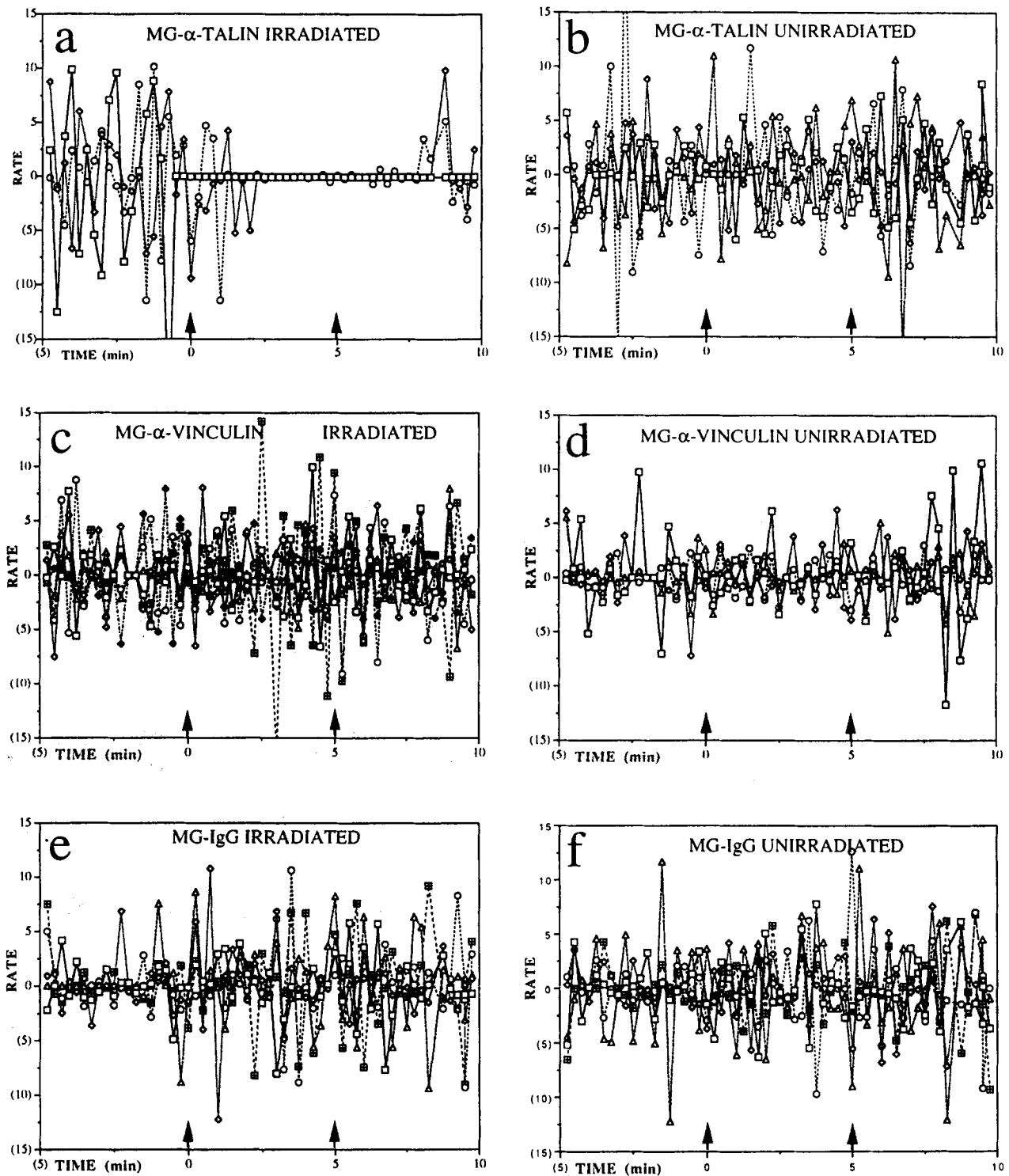
Figure 6. Micro-CALI of talin causes a cessation of filopodial extension and retraction. The rates of extension and retraction for all irradiated and all unirradiated filopodia on a given growth cone are plotted vs time over a 15-min time-lapse period. The start and end of laser irradiation is denoted by arrowheads. (*a* and *b*) Micro-CALI of talin caused a loss of motility. During laser irradiation, the rates of all irradiated filopodia (*a*) drop to 0.0 ± 0.2 μm/min for 5.5 min, after which time, motility is recovered. The rates of extension and retraction for unirradiated filopodia of the same growth cone (*b*) varied dynamically throughout the time-lapse period. (*c–f*) No significant change in the rates of motility was seen after micro-CALI of vinculin (*c* and *d*) or MG-IgG controls (*e* and *f*) regardless of laser irradiation.
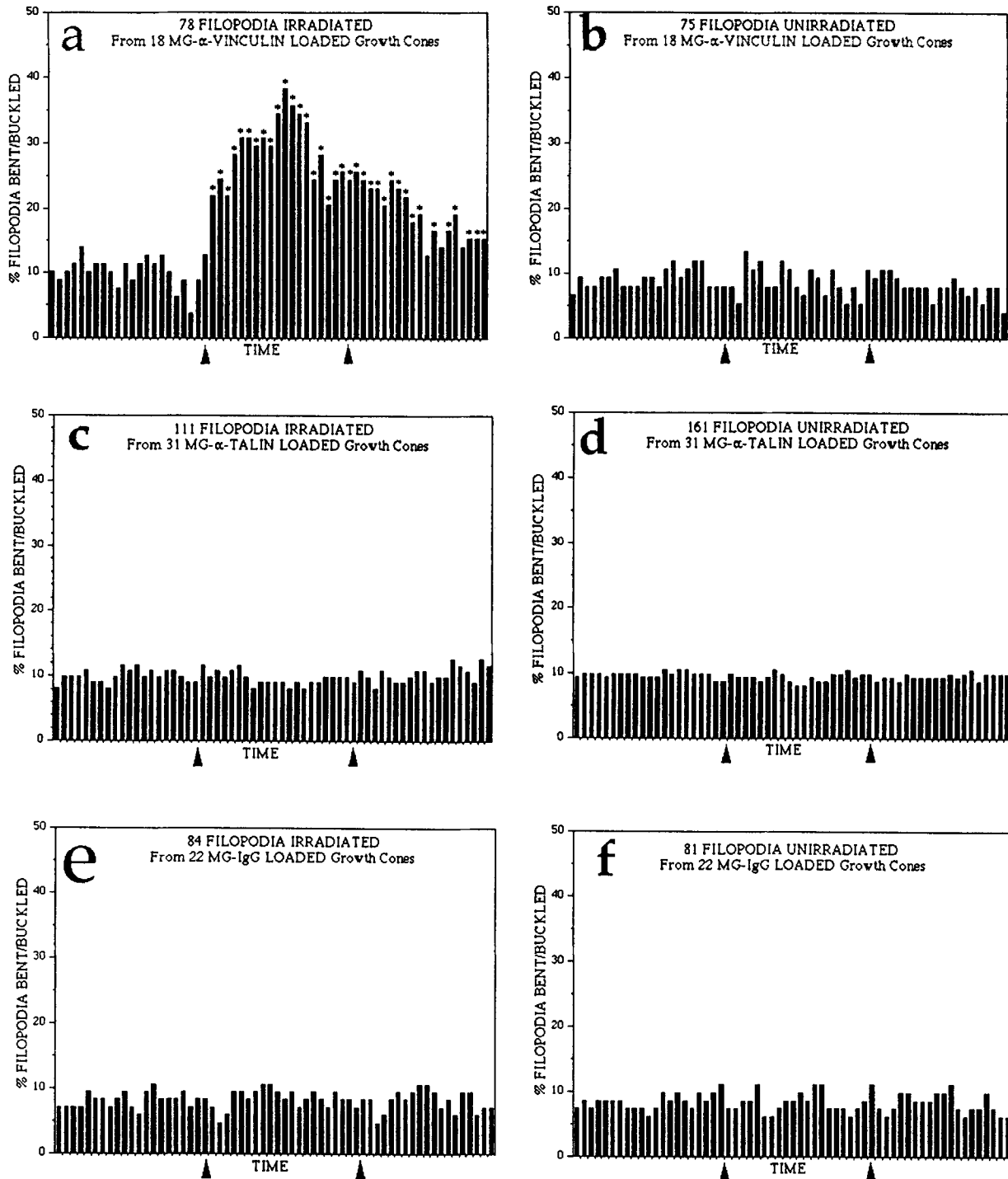
Figure 7. Micro-CALI of vinculin causes filopodial bending and buckling. The number of filopodia that bent or buckled at each 15-s time point in the 15-min time-lapse period was pooled for all irradiated and unirradiated filopodia on growth cones that received the same micro-CALI treatment to obtain the percentage of bending and buckling at each time point. A baseline 10% of filopodia was bent or buckled before laser irradiation (*left of first arrowhead*). *, a significant difference from the baseline average (zM test, $P < 0.05$). (*a* and *b*) Micro-CALI of vinculin caused a significant increase to 35–40% bending and buckling of irradiated filopodia (*a*) that gradually decreased toward baseline after laser irradiation (*right of second arrowhead*). Unirradiated filopodia (*b*) showed no significant increase in bending and buckling above baseline levels. (*c–f*) Micro-CALI of talin (*c* and *d*) or MG-IgG controls (*e* and *f*) showed no significant change in bending and buckling regardless of laser irradiation.

experiments were done and analyzed (focal plane at the surface of the coverslip), it was only possible to track attached filopodia, as these were the only ones in focus throughout the time lapse.

Filopodia extend and retract dynamically, and net growth must depend on the relative ratio of the two. That both extension and retraction cease after talin inactivation suggests that movement in both directions is dependent on talin. It is known that filopodia are held in tension (Bray, 1979), and the counteracting rearward and forward forces may act simultaneously at focal contacts. In this way, talin may play a crucial role as the fulcrum in the balance of forces during filopodial movement. This role makes the regulation of talin–integrin binding by tyrosine phosphorylation (Tapley et al., 1989; Schmidt et al., 1993) particularly interesting as a means of regulating filopodial motility. Localized interactions with extracellular cues could regulate tyrosine phosphorylation at this site (Atashi et al., 1992; Rivas et al., 1992), and thereby locally modulate the efficacy of the coupling of motility to actin dynamics.

Several models for filopodial motility have been put forth (Oster and Perelson, 1987; Mitchison and Kirschner, 1988; Sheetz et al., 1992). All of these require that the F-actin is fixed in position to either couple motility to actin dynamics or molecular motors (Mitchison and Kirschner, 1988; Sheetz et al., 1992), or as a barrier to allow the generation of osmotic pressure (Oster and Perelson, 1987). Our data are consistent with talin acting to hold the F-actin in place with respect to the filopodium and the external environment but do not distinguish between these models.

The CALI-induced cessation of filopodial motility did not result in either a change in neurite outgrowth or growth cone turning when micro-CALI was done asymmetrically. This is in contrast with the effects previously observed when calcineurin was regionally inactivated (Chang et al., 1995). Filopodial motility is known to be important for neurite extension and growth cone turning (O'Connor et al., 1990; Marsh and Letourneau, 1984; Bentley and Toroian-Raymond, 1986; Forscher and Smith, 1988). The transient stalling of filopodia resulting from micro-CALI of talin is not sufficient to influence subsequent growth cone motility or neurite extension.

Our findings suggest that vinculin has a role in the structural integrity of the filopodia. Bending and buckling is commonly observed at low frequency, but we demonstrated the increased incidence of this behavior by summing the filopodia from a population of growth cones correlated with respect to the initiation time and site of laser irradiation. This type of analysis may be generally useful in observing trends in growth cone behavior in response to precisely timed stimuli.

Previous studies that generated loss of vinculin have observed a change in motility in PC12 cells (Varnum-Finney and Reichardt, 1995) and in fibroblasts (Samuels et al., 1993; Rodriguez-Fernandez et al., 1993), but the loss of vinculin mediated by antisense RNA in these two cell types caused opposite effects on motility. This suggests that the role of vinculin in motility is complex. Micro-CALI of vinculin in the filopodia resulted in bending and buckling, and this is consistent with the observation of unstable filopodia in the PC12 cell experiments (Varnum-Finney and Reichardt, 1995), but we did not observe a change in filopodial or neurite extension. Our data showed that a short-term loss of vinculin in growth cone filopodia does not affect motility. These other studies generate a long-term change in vinculin function that may cumulatively alter motility.

Adhesion of filopodia has been suggested to explain filopodial buckling during outgrowth of mouse cerebral cortex neurons (Sheetz et al., 1992), and vinculin may function in adhesion as a component of focal contacts. Alternatively, vinculin binding to F-actin may bundle microfilaments to stabilize filopodial structure. The mutiple F-actin binding sites on vinculin and its ability to bundle F-actin in vitro support this hypothesis (Johnson and Craig, 1995). As filopodia are held under tension (Bray, 1979), CALI may cause a weakening of vinculin-mediated focal contacts or a decrease of actin bundling within a filopodium that would result in a tension-mediated bending or buckling at its weakest point.

The distinct growth cone motile behaviors in response to micro-CALI of talin and vinculin are a demonstration of the specificity of CALI for associated proteins inside growth cones. It is consistent with the spatial specificity of CALI shown in previous work in vitro (Linden et al., 1992; Liao et al., 1994) and in vivo (Liao et al., 1995). Other micro-CALI experiments directed to growth cone proteins such as calcineurin (Chang et al., 1995) show markedly different growth cone behaviors in response to localized inactivation of these proteins. These differential effects when CALI is directed to different proteins support the specificity of CALI and demonstrate its use in addressing protein function during growth cone motility and guidance. We believe that the approach and analysis presented here will also be useful in elucidating other cellular mechanisms.

References

Atashi, J.R., S.G. Klinz, C.A. Ingraham, W.T. Matten, M. Schachner, and P.F. Maness. 1992. Neural cell adhesion molecules modulate tyrosine phosphorylation of tubulin in nerve growth cone membranes. *Neuron.* 8:831–842.

Beermann, A.E., and D.G. Jay. 1994. Chromophore-assisted laser inactivation of cellular proteins. *Methods Cell Biol.* 44:716–732.

Bentley, D., and A. Toroian-Raymond. 1986. Disoriented pathfinding by pioneer neurone growth cones deprived of filopodia by cytochalasin treatment. *Nature (Lond.).* 323:712–715.

Borasio, G.D., J. John, A. Wittinghofer, Y.A. Barde, M. Sendtner, and R. Heumann. 1989. ras p21 protein promotes survival and fiber outgrowth of cultured embryonic neurons. *Neuron.* 2:1087–1096.

Bray, D. 1979. Mechanical tension produced by nerve cells in tissue culture. *J. Cell Sci.* 37:391–410.

Bray, D. 1991. Isolated chick neurons for the study of axon growth. *In* Culturing Nerve Cells. G. Banker and K. Goslin, editors. MIT Press, Cambridge, MA. 104–120.

Burridge, K., and P. Mangeat. 1984. An interaction between vinculin and talin. *Nature (Lond.).* 308:744–746.

Burridge, K., K. Fath, T. Kelly, G. Nuckolls, and C. Turner. 1988. Focal adhesion: transmembrane junctions between the extracellular matrix and the cytoskeleton. *Annu. Rev. Cell Biol.* 4:487–525.

Chang, H.Y., K. Takei, A.M. Sydor, T. Born, F. Rusnak, and D.G. Jay. 1995. Asymmetric retraction of growth cone filopodia follows focal inactivation of calcineurin. *Nature (Lond.).* 376:686–690.

Chien, C.B., D.E. Rosenthal, W.A. Harris, and C.E. Holt. 1993. Navigational errors made by growth cones without filopodia in the embryonic *Xenopus* brain. *Neuron.* 11:237–251.

Clarke, M., and P. McNeil. 1992. Syringe loading introduces macromolecules into living mammalian cell cytosol. *J. Cell Sci.* 102:533–541.

Diamond, P., A. Mallavarapu, J. Schnipper, J. Booth, L. Park, T.P. O'Connor, and D.G. Jay. 1993. Fasciclin I and II have distinct roles in the development of grasshopper pioneer neurons. *Neuron.* 11:409–421.

Dubreuil, R., T.J. Byers, D. Branton, L.S.B. Goldstein, and D.P. Kiehart. 1987. *Drosophila* spectrin. I. Characterization of the purified protein. *J. Cell Biol.* 105:2095–2102.

Forscher, P., and S. Smith. 1988. Actions of cytochalasins on the organization of actin filaments and microtubules in a neuronal growth cone. *J. Cell Biol.* 107:1505–1516.

Gilmore, A.P., C. Wood, V. Ohanian, P. Jackson, B. Patel, D.J.G. Rees, R.O. Hynes, and D.R. Critcheley. 1993. The cytoskeletal protein talin contains at least two distinct vinculin binding domans. *J. Cell Biol.* 122:337–347.

Horwitz, A.F., K. Duggan, C. Buck, M.C. Berkerle, and K. Burridge. 1986. Interactions of plasma membrane fibronectin receptor with talin—a transmembrane linkage. *Nature (Lond.).* 320:531–533.

Jay, D.G. 1988. Selective destruction of protein function by chromophore-assisted laser inactivation. *Proc. Natl. Acad. Sci. USA.* 85:5454–5458.

Jay, D.G., and H. Keshishian. 1990. Laser inactivation of fasciclin I disrupts axon adhesion of grasshopper pioneer neurons. *Nature (Lond.).* 348:548–550.

Johnson, R.P., and S.W. Craig. 1995. F-actin binding site masked by the intramolecular association of vinculin head and tail domains. *Nature (Lond.).* 373:261–264.

Letourneau, P.C. 1983. Differences in the organization of actin in the growth cones compared with the neurites of cultured neurons from chick embryos. *J. Cell Biol.* 97:963–973.

Letourneau, P.C. 1992. Integrins and n-Cadherin are adhesive molecules involved in growth cone migration. *In* The Nerve Growth Cone. P.C. Letourneau, S.B. Kater, and E.R. Macagno, editors. Raven Press, New York. 181–194.

Letourneau, P.C., and T. M. Gomez. 1996. DRG growth cones make focal contacts on fibronectin-treated substrata. *J. Neurobiol.* In press.

Letourneau, P.C., and T.A. Shattuck. 1989. Distribution and possible interactions of actin-associated proteins and cell adhesion molecules of nerve growth cones. *Development (Camb.).* 105:505–519.

Liao, J.C., J. Roider, and D.G. Jay. 1994. Chromophore-assisted laser inactivation of proteins is mediated by the photogeneration of free radicals. *Proc. Natl. Acad. Sci. USA.* 91:2659–2663.

Liao, J.C., L.J. Berg, and D.G. Jay. 1995. Chromophore-assisted laser inactivation of subunits of the T cell receptor in living cells is spatially restricted. *Photochem. Photobiol.* 62:923–929.

Linden, K., J.C. Liao, and D.G. Jay. 1992. Spatial specificity of chromophore-assisted laser inactivation of protein function. *Biophys. J.* 61:956–962.

Marsh, L., and P.C. Letourneau. 1984. Growth of neurites without filopodial or lamellipodial activity in the presence of cytochalasin B. *J. Cell Biol.* 99:2041–2047.

Mitchison, T., and M. Kirschner. 1988. Cytoskeletal dynamics and nerve growth. *Neuron.* 1:761–772.

Molony, L., D. McCaslin, J. Abernethy, B. Paschal, and K. Burridge. 1987. Properties of talin from chicken gizzard smooth muscle. *J. Biol. Chem.* 262:7790–7795.

Nuckolls, G.H., L.H. Romer, and K. Burridge. 1992. Microinjection of antibodies against talin inhibits the spreading and migration of fibroblasts. *J. Cell Sci.* 102:753–762.

O'Connor, T.P., J.S. Duerr, and D. Bentley. 1990. Pioneer growth cone steering decisions mediated by single filopodial contacts in situ. *J. Neurosci.* 10:3935–3946.

Oster, G.F., and A.S. Perelson. 1987. Role of osmotic pressure in cell extension. *J. Cell Sci. Suppl.* 8:35–53.

Otey, C., W. Griffith, and K. Burridge. 1990. Characterization of monoclonal antibodies to chicken gizzard talin. *Hybridoma.* 9:57–62.

Rivas, R.J., D.W. Burmeister, and D.J. Goldberg. 1992. Rapid effects of laminin on the growth cone. *Neuron.* 8:107–115.

Rodriguez-Fernandez, J.L., B. Geiger, D. Salomon, and A. Ben-Ze'ev. 1992. Overexpression of vinculin suppresses cell motility in BALB/c 3T3 cells. *Cell Motil. Cytoskeleton.* 22:127–134.

Rodriguez-Fernandez, J.L., B. Geiger, D. Salomon, and A. Ben-Ze'ev. 1993. Supression of vinculin expression by antisense transfection confers changes in cell morphology, motility, and anchorage-dependent growth of 3T3 cells. *J. Cell Biol.* 122:1285–1294.

Samuels, M., R.M. Ezzell, T.J. Cardozo, D.R. Critchley, J.L. Coll, and E.D. Adamson. 1993. Expression of chicken vinculin complements the adhesion-defective phenotype of a mutant mouse F9 embryonal carcinoma cell. *J. Cell Biol.* 121:909–921.

Samuelsson, S.J., P.W. Luther, D.W. Pumplin, and R.J. Bloch. 1993. Structures linking microfilament bundles to the membrane at focal contacts. *J. Cell Biol.* 122(2):485–496.

Schmidt, C.E., A.F. Horwitz, D.A. Lauffenburger, and M.P. Sheetz. 1993. Integrin–cytoskeletal interactions in migrating fibroblasts are dynamic, asymmetric, and regulated. *J. Cell Biol.* 123:977–991.

Sheetz, M.P., D.B. Wayne, and A.L. Pearlman. 1992. Extension of filopodia by motor-dependent actin assembly. *Cell Motil. Cytoskeleton.* 22:160–168.

Stossel, T.P. 1993. On the crawling of animal cells. *Science (Wash. DC).* 260:1086–1094.

Tapley, P., A.F. Horwitz, C. Buck, K. Duggan, and L. Rohrschneider. 1989. Integrin isolated from Rous sarcoma virus-transformed chicken embryo fibroblasts. *Oncogene.* 4:325–333.

Varnum-Finney, B., and L. Reichardt. 1994. Vinculin-deficient PC12 cell lines extend unstable lamellipodia and filopodia and have a reduced rate of neurite outgrowth. *J. Cell Biol.* 127:1071–1084.

Wachsstock, D.H., J.A. Wilkins, and S. Lin. 1987. Specific interaction of vinculin with α-actinin. *Biochem. Biophys. Res. Commun.* 146:554–560.

Westmeyer, A., K. Ruhnau, A. Wegner, and B.M. Jockusch. 1990. Antibody mapping of functional domains in vinculin. *EMBO (Eur. Mol. Biol. Organ.) J.* 9:2071–2078.

Yamada, K.M., B.S. Spooner, and N.K. Wessels. 1970. Axon growth: role of microfilaments and microtubules. *Proc. Natl. Acad. Sci. USA.* 66:1206–1212.

Zheng, J.Q., J.J. Wan, and M.M. Poo. 1996. Essential role of filopodia in chemotropic turning of nerve growth cone induced by a glutamate gradient. *J. Neurosci.* 16:1140–1149.